physical sciences forum

MDPI

Proceeding Paper

Heating Kinetics of Gold Nanoparticles in Biological Tissues with a Femtosecond Laser †

Selma Mediene * and Assia Rachida Senoudi

Physics Department, Theoretical Physics Laboratory, Tlemcen University, Tlemcen 13000, Algeria
* Correspondence: selma.mediene@uinv-tlemcen.dz or selmamediene@gmail.com
† Presented at the 1st International Conference on Physics of Semiconductor Devices, Renewable Energies and Environment, Bechar, Algeria, 14–16 November 2022.

Abstract: This work deals with a numerical study of the different thermal processes in a gold nanoparticle heated with a femtosecond pulse laser and cooled in different biological tissues, such as healthy human prostate, blood, fat, tumor prostate, skin and protein myoglobin. A 40 nm diameter gold nanoparticle is heated using a femtosecond pulse laser with a duration of 85 fs and a fluence of 1.4 J/m^2. A two-temperature model is used to describe the dynamics of the exchange of energy between the electron gas and the phononic lattice in addition to Fourier's law and the relationship between the thermal conductivity of the external medium and the temperature. The temperature of the external medium near the nanoparticle surface was computed, and the effect of the laser energy was reported.

Keywords: gold nanoparticle; ultra-short pulse laser; heat flux dissipation; two-temperature model; fourth-order Runge–Kutta scheme

1. Introduction

The interaction between nanomaterials and ultra-short pulse lasers has been investigated considerably in recent years and has showed extraordinary properties [1–5]. Several researchers showed that at the nanoscale, physical, chemical and electronic properties of nanoparticles are very different compared with those of bulk gold. The most remarkable properties are the optical and thermal properties of metallic nanoparticles, particularly gold nanoparticles (GNPs), which absorb strongly photonic energy at visible or infrared frequencies when they are smaller than 100 nm in size due to their localized surface plasmon resonance [6].

The field of the applications of these proprieties is expansive, especially in nano-optics [7,8], biology and nanomedicine [9,10]. The dynamics of thermal relaxation in GNPs offer them the ability to be localized and highly thermal sources for damaging cancer cells. GNPs injected into biological media provide a highly selective method for causing damage to abnormal cells (e.g., cancer tumor) when they are irradiated with the appropriate laser pulse duration. The amount of heat generated by a plasmonic GNP can be controlled by the particle size, shape and aggregation state of the GNP as well as the illuminating laser intensity, wavelength and pulse duration.

A GNP is composed of two distinct subsystems, specifically electrons and phonons. The photons emitted from a femtosecond laser pulse are first absorbed by free electrons via inverse bremsstrahlung, transferred to the lattice subsystem by electron–phonon scattering, and then transferred to the surrounding medium [11]. Thermal equilibrium between the electron gas and the metallic lattice is achieved in a few tens of picoseconds. As the lattice temperature increases, the heat loss from the particle to its surrounding medium occurs through phonon–phonon coupling in a few nanoseconds. The heat transfer from the GNP to the medium can lead to the formation of a photothermal bubble in liquid [12].

Citation: Mediene, S.; Senoudi, A.R. Heating Kinetics of Gold Nanoparticles in Biological Tissues with a Femtosecond Laser. *Phys. Sci. Forum* **2023**, *6*, 1. https://doi.org/10.3390/psf2023006001

Academic Editor: Mebarka Daoudi

Published: 24 March 2023

It is important to study the exchange of energy in metallic nanoparticles between electrons and phonons while taking into consideration the dependence of temperature in the electron–phonon coupling factor. To study this fast thermal process, we proposed to use a two-temperature model (TTM), which provides a good description of the thermal kinetics of GNPs [13–17]. The TTM is a system of two coupled and nonlinear differential equations, one describing the temporal evolution of the electron gas and the other describing the phononic lattice in a response to a pulse laser. Mathematically, the dynamics of these processes are modeled using the Anisimov two-temperature model and the numerical solution of the Navier–Stokes equations [11,18].

In the present work, we have numerically studied the heating kinetics of a spherical, 40 nm diameter GNP cooled in various biological tissues, such as water, healthy human prostate, blood, fat, tumor prostate, skin and protein myoglobin, under a femtosecond laser with an incident laser beam of wavelength λ = 550 nm. The time duration is τ_p = 85 fs and the fluence is F_P = 1.4 J/m^2, which is comparable to the experimental data in [19]. The use of a GNP with a diameter between 10 and 40 nm in rapid hyperthermia seems adequate and effective at the protein level since biological systems, such as cells (1–10 μm), proteins (1–10 nm) and bacteria (1–10 mm), are characterized by a wide range of sizes [20].

This numerical predictive study will be presented by taking into account the electron–phonon relaxation time for the GNP, the interface conductance between the particle and its surroundings, the diffusion of the heat from the GNP to the surrounding medium and the amount of energy absorbed by the biological tissues. Conduction losses are a function of the thermal interface conductance of the gold and the temperature at the GNP/surrounding media interface. In order to determine the latter, Ekici [14] solved the heat diffusion equation in the water as a third equation using the finite difference method in addition to the TTM equations. However, in our work, we have simply used Fourier's law and the relationship between the thermal conductivity of the external medium and the temperature.

Mie theory gives not only the integral characteristics of the interaction between plane diffusion waves and spherical particles but also the absorption A_{abs}, the scattering A_{scat} and the extinction A_{ext} cross-sections [6]. The computer calculation of theses quantities for a spherical GNP in a wide range of radiuses and for some laser wavelengths can be performed using a Fortran code, as in [21]. Two physical quantities are necessary for computing the A_{abs} required in the calculation of the photonic energy absorbed by the GNP, specifically the refractive indexes of the GNP and the external media. These quantities depend, in general form, on the light wavelength.

We resolve the TTM numerically with a Fortran program that we have devised by using a fourth-order Runge–Kutta algorithm [22], which is convergent and accurate.

2. Theoretical Study

We consider a spherical, 40 nm diameter GNP immersed first in water (the external environment is varied thereafter). The GNP is heated with a femtosecond pulse laser and assumed uniformly illuminated at its plasmonic frequency. The electron and phonon temperature relaxation and the electron–phonon coupling inside the spherical GNP were represented on the basis of two coupled kinetic equations, as shown in Equation (1). The first equation describes the thermal transfer between the electron gas energy and the lattice, and the second describes the heating of the lattice:

$$\begin{cases} C_e \frac{dT_e}{dt} = -g(T_e - T_L) + S(t) \\ C_L \frac{dT_L}{dt} = g(T_e - T_L) - Q(t) \end{cases} \quad (1)$$

T_e and T_L are the temperatures of the electron gas and the lattice, respectively, and C_e and C_L are the specific heats per unit of volume of the electrons and phonons, respectively. In general, C_e and C_L depend on T_e and T_L. The electron–phonon coupling is represented by the factor. The term $S(t)$ represents the laser energy deposition into the electron subsystem of the GNP per unit of time and per unit of volume. $Q(t)$ represents the released heat power

from the particle to its surrounding medium per unit of volume. The heat loss includes, in general form, the energy losses due to heat conduction (Q_C) and radiation cooling (Qr). However, radiation transfer is not included in our calculations because it is much smaller than Q_C for temperatures $T < 5000$ K [2]. Finally, t represents the time. The thermophysical parameters of the GNP are given in Table 1.

Table 1. Thermophysical parameters of the GNP.

Parameters	Unit (SI)	Value	Ref.
The electron heat capacity, C_e	J/(Km^3)	$C_e = 70 \times T_e$	[17]
The lattice heat capacity, C_L	J/(Km^3)	$C_L = \rho_{gold} \times (109.707\ T_L - 3.4 \times 10^{-4} {T_L}^2 + 5.24 \times 10^{-7} {T_L}^3 - 3.93 \times 10^{-10} {T_L}^4 + 1.17 \times 10^{-13} {T_L}^5 t)$	[14]
Density, ρ_{gold}	Kg/m^3	$\rho_{gold} = 1.93 \times 10^4$	[17]
Electron–lattice coupling coefficient, g	W/(Km^3)	$g = 2.2 \times 10^{16}$	[9]
Thermal conductance, G	W/(Km^2)	$G = 105 \times 10^6$	[14]

The source term $S(t)$, as shown in Equation (2), has a Gaussian temporal profile $f(t)$ and an exponential spatial damping, as shown in Equation (3):

$$S(t) = \frac{1}{V_P} \frac{A_{abs} \times F_P}{\tau_P} \times f(t) \tag{2}$$

$$f(t) = \frac{2\sqrt{ln(2)}}{\sqrt{\pi}} e^{-4ln(2) \times \left(\frac{t-2\tau_P}{\tau_P}\right)^2} \tag{3}$$

V_p represents the volume of the GNP, τ_p is the full width at half maximum of the laser pulse and F_p represents the laser fluence.

According to [1,2], heat loss by conduction is given by Equation (4), with T_S representing the temperature at the interface of the GNP/biological tissue:

$$Q_C = \frac{S_p}{R} \int_{T_\infty}^{T_s} k(T) dT \tag{4}$$

$S_p = 4\pi R^2$ represents the area of the GNP, R its radius and $k(T)$ the thermal conductivity of the external medium.

The thermal conductivity of the external medium can be written as a power law temperature function given in the following form: $k(T) = k_\infty\ (T/T_\infty)^a$ [2]. k_∞ represents the thermal conductivity of the surrounding medium at $T = 25$ °C, and T_∞ is the initial temperature of the GNP and the surrounding media. The constant a depends on the thermal properties of the surrounding medium, and for a biological medium, we put $a = 1$ according to [1]. The conductivity of water at $T_\infty = 300$ K is $k_\infty = 0.61$ W/Km. The surrounding media corresponding to some biological tissues are characterized by different thermal conductivities k_∞ and different optical refractive indexes (Table 2).

We assume the continuity of the temperature at the interface of the GNP/surrounding medium; therefore, we can write $T_S = T_L$, and after the integration of Equation (4), we found the following:

$$Q_C = 2\pi R k_\infty T_\infty \left(\left(\frac{T_L(t)}{T_\infty} \right)^2 - 1 \right) \tag{5}$$

We resolve the TTM numerically by using a fourth-order Runge–Kutta algorithm with following initial conditions: $T_e(t = 0) = T_L(t = 0) = T_\infty$. The time step of the simulation is in picoseconds.

Table 2. Thermophysical and optical proprieties of different biological tissues.

Biological Tissues	Thermal Conductivity k_∞ (W/m/K) [8]	Refractive Indexes	References	Computed Optical Absorption A_{abs} Cross-Section (nm^2)
Protein myoglobin	0.15	1.35	[23] Kurisaki	3831.29
Human prostate	0.529	1.40	[24] DeLunaa	4375.18
Blood	0.48–0.6	1.37	[25] Elblbesy	4045.33
Fat	0.23	1.47	[26] Bacallao	5064.83
Tumor prostate	0.45	1.35	[24] DeLunaa	3829.58
Skin	0.210–0.410	1.46	[27] Ding	5064.83
Water	0.61	1.33	[14] Ikici	3623.83

The temperature of the water near the GNP surface, noted as T_{ws}, can be computed from the following relation [13]:

$$Q_C = G\, S_p(\, T_L(t) - T_{ws}(t)) \tag{6}$$

G represents the interfacial thermal conductance, which links the temperature drop at the interface to the heat flux crossing the interface. The size dependence of the thermal conductance may be described by the empirical relation proposed in [28,29], as $G(R) = G_\infty\,(1 + \delta/R)$ and G_∞ represent the value of the infinite radius thermal conductance and δ represents the characteristic length on the order of a molecular size.

3. Numerical Results

Figure 1 gives the plots for the optical cross-sections of the GNP embedded in water with a light wavelength. The plasmon resonance occurs at 524 nm. The shift in this resonance frequency is due to the electron gas heating and population changes near the Fermi level, leading to an increased probability of 5d–6sp transition in the GNP.

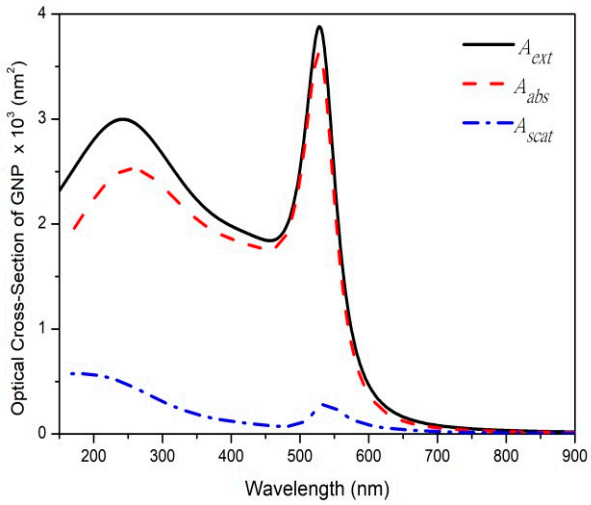

Figure 1. Extinction (A_{ext}), absorption (A_{abs}), scattering (A_{scat}) cross-sections as functions of wavelength calculated using Mie code for the 40 nm diameter GNP embedded in water.

Figure 2 exhibits the thermal responses of both the electron gas and the gold lattice when the 40 nm diameter GNP is heated with a femtosecond laser and cooled in water. The pulse duration is τ_p = 85 fs and the fluence is F_P = 1.4 J/m^2. The electron–lattice coupling is achieved at approximately 10 ps. The GNP reaches a temperature of 331 K, and the cooling time of the GNP is found to be 2 nanoseconds.

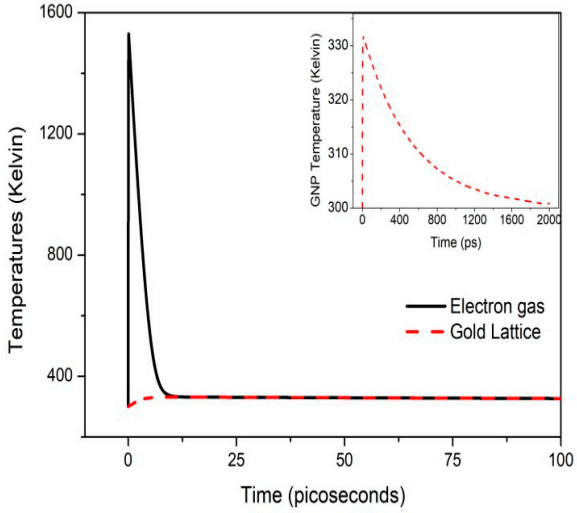

Figure 2. Simulated temporal evolution of electron temperature, T_e (solid black line), and GNP temperature, T_L (dashed red line), of the 40 nm diameter GNP heated with a femtosecond pulse laser and cooled in water. Duration time is 85 fs and fluence is 1.4 J/m^2. The inset shows the temporal evolution of the GNP temperature.

Figure 3 shows the temperature of the GNP when cooled in different biological tissues, such as human prostate, blood, fat, tumor prostate, skin and water. The heating of the GNP is more intense in skin and fat than in the other tissues.

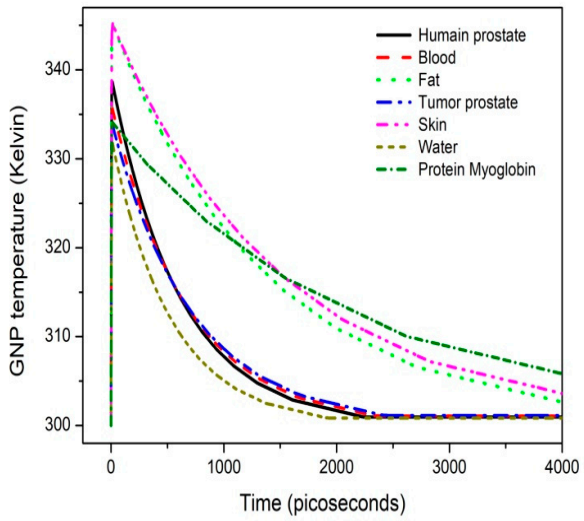

Figure 3. Temporal evolution of temperature of the GNP cooled in different biological tissues (human prostate, blood, fat, tumor prostate, skin, water and protein myoglobin). Duration time is 85 fs and fluence is 1.4 J/m^2.

Figure 4 gives the temporal evolutions of both the temperatures of the GNP and the water near the GNP surface. These curves showed an increase of 30 °C in the GNP temperature and 20 °C in T_{ws} with a laser heating of 1.4 J/m^2. Gan et al. found an increase of 30 °C in T_{ws} with the same fluence for a 120 × 40 nm^2 gold nanorod [17].

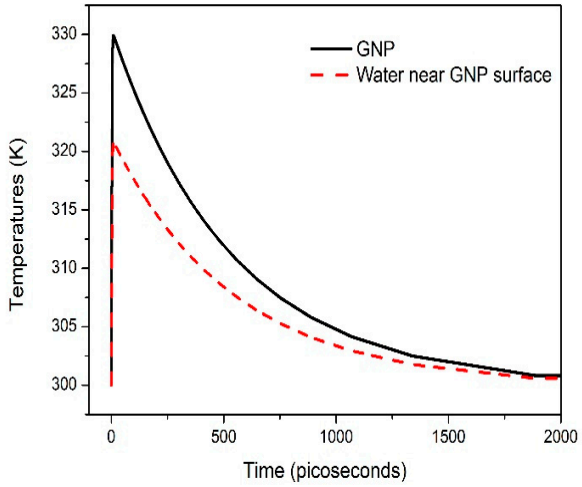

Figure 4. Temporal evolution of the GNP temperature (solid line) and the water temperature near the GNP surface (dashed line). Duration time is 85 fs and fluence is 1.4 J/m^2.

We will show in a future work that it is not necessary to increase the laser fluence to increase the temperature of the GNP; however, a sequence of sub-pulses (adequately separated) from a burst femtosecond laser is sufficient to produce a fast heat accumulation in the GNP and in the external medium near the interface without increasing the laser energy.

Figure 5 shows the increasing maximum temperatures of the different biological tissues near the GNP surface as a function of laser fluence within a range (0.1–1.4) J/m^2 at the same pulse duration. The rates of temperature increase in skin, fat, protein myoglobin, human prostate, blood, tumor prostate and water are 27.08, 26.76, 21.14, 18.97, 18.16, 17.57 and 14.83 K per J/m^2, respectively. The temperatures near the GNP surface in fat and skin are more intense and decrease slowly compared with the other biological tissues. This conclusion (concerning the fat) is similar to that found [1], where Lutfellin et al. used a one-temperature model in their calculations and found a higher overheating for a 30 nm diameter GNP embedded in fat with a 100 J/m^2 fluence and an 8 ns duration. The curves in Figure 5 can indicate the threshold fluences for the melting point (which is T_m~1337 K for gold bulk and is between 800 and 900 K for a 3 nm GNP, as shown in [28]), the boiling temperature (T_b~3130 K), the critical temperature of water (T_{cr}~647 K), as reported in [30], and the cavitation threshold of water (T_{cav}~573 K) [18].

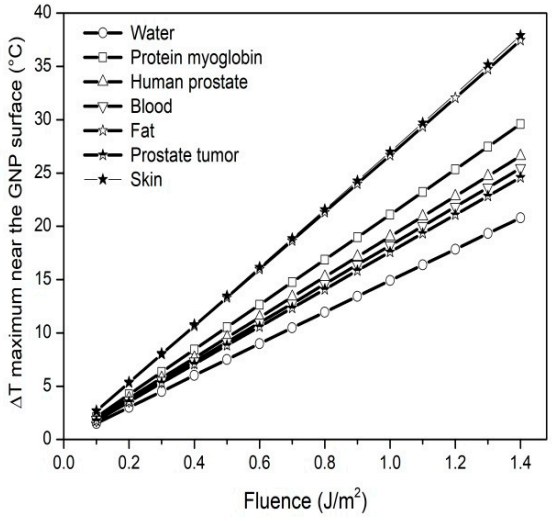

Figure 5. The relationship between the maximum temperatures of different biological tissues near the GNP surface and the laser fluence. Duration time is 85 fs.

It should be said that nanoparticles can react selectively with the host medium depending on a set of conditions related to the nature of the particles and the biological tissue. The particles placed within a human body must be functionalized and can carry molecules that could be hydrophobic or hydrophilic, which react differently. There are other effects that must be taken into account to define the appropriate choice of laser parameters and GNP properties for the effective therapy of tumor tissues [20].

4. Conclusions

In this work, we investigated numerically the dynamics of the ultra-rapid exchange of energy in a spherical GNP immersed in different biomedia and heated at their plasmonic resonances using a femtosecond pulse laser. The temperatures near the GNP surface in fat and skin are more intense and decrease slowly compared with the other biological tissues. The surrounding environments of the GNP are the biological tissues. It would be interesting to complete the modeling by incorporating the bio-Pennes equation. Our numerical study has only been concerned with a single GNP heated by a single pulse; thus, it seems judicious to complete the mathematical formalism by including a multipulse laser as well as the distribution of the nanoparticles in the medium in order to establish adequate conclusions. This will be done in a future work.

Author Contributions: Conceptualization, S.M.; methodology, S.M.; software, A.R.S.; validation, A.R.S.; formal analysis, S.M. and A.R.S.; investigation, S.M.; resources, S.M.; writing—original draft preparation, S.M.; writing—review and editing, A.R.S.; visualization, A.R.S.; supervision, A.R.S.; project administration, A.R.S. All authors have read and agreed to the published version of the manuscript.

Funding: This research received no external funding.

Institutional Review Board Statement: Not applicable.

Informed Consent Statement: Not applicable.

Data Availability Statement: Not applicable.

Conflicts of Interest: The authors declare no conflict of interest.

References

1. Letfullin, R.R.; George, T.F.; Duree, G.C.; Bollinger, B.M. Ultrashort Laser Pulse Heating of Nanoparticles: Comparison of Theoretical Approaches. *Adv. Opt. Technol.* **2008**, *2008*, 251718. [CrossRef]
2. Pustovalov, K.V. Theoretical study of heating of spherical nanoparticle in media by short laser pulses. *Chem. Phys.* **2008**, *308*, 103–108. [CrossRef]
3. Fasla, F.; Senoudi, A.R.; Boussaid, A.; Benmouna, M.; Benmouna, R. Heating of Biological Tissues by Gold Nano Particles: Effects of Particle Size and Distribution. *J. Biomat. Nanobiotech.* **2011**, *2*, 49–54. [CrossRef]
4. Guillaume, B.; Herve, R. Femtosecond pulsed optical heating of gold nanoparticles. *Phys. Rev. B* **2011**, *84*, 035415.
5. Wang, X.; Xu, X. Thermo elastic wave in metal induced by ultrafast laser pulses. *J. Ther. Stress.* **2002**, *25*, 457–473. [CrossRef]
6. Bohren, C.F.; Huffman, D.R. *Absorption and Scattering of Light by Small Particles*; Wiley-Interscience: New York, NY, USA, 1983.
7. French, P.M.W.; Williams, J.A.R.; Taylor, J.R. Passively mode locked c.w. dye lasers operating from 490 nm to 800 nm. *Revue Phys.* **1987**, *22*, 1651–1655. [CrossRef]
8. Dmitriev, P.A.; Makarov, S.V.; Milichko, V.A.; Mukhin, I.S.; Samusev, A.K.; Krasnok, A.E.; Belov, P.A. Direct femtosecond laser writing of optical Nanoresonators. *J. Phys.* **2016**, *690*, 012021. [CrossRef]
9. Jain, S.; Hirst, D.G.; O'Sullivan, J.M. Gold nanoparticles as novel agents for cancer therapy. *Br. J. Radiol.* **2012**, *85*, 101–113. [CrossRef]
10. Pitsillides, C.M.; Joe, E.K.; Wei, X.; Anderson, R.R.; Charles, P.; Lin, C.P. Selective Cell Targeting with Light-Absorbing Microparticles and Nanoparticles. *Biophys. J.* **2003**, *84*, 4023–4032. [CrossRef]
11. Anisimov, I.S.; Kapeliovich, B.L.; Perel'man, T.L. Electron emission from metal surfaces exposed to ultrashort laser pulses. *Soviet Phys. JETP* **1974**, *39*, 375–377.
12. Hashimoto, S.; Werner, D.; Uwada, T. Studies on the interaction of pulsed lasers with plasmonic gold nanoparticles toward light manipulation, heat management, and nanofabrication. *J. Photochem. Photobiol. C Photochem. Rev.* **2012**, *13*, 28–54. [CrossRef]
13. Jing, H.; Kapil, B.; Chen, J.K.; Zhang, Y. An axisymetric model for solid-liquid-vapor change in thin metal films induced by an ultrashort laser pulse. *Front. Heat Mass Transf.* **2011**, *2*, 013005.

14. Ekici, O.; Harrison, R.K.; Durr, N.J.; Eversole, D.S.; Lee, M.; Ben-Yakar, A. Thermal analysis of gold nanorods heated with femtosecond laser pulses. *J. Phys. D Appl. Phys.* **2008**, *4*, 185501. [CrossRef]
15. Bresson, P.; Bryche, J.F.; Besbes, M.; Moreau, J.; Karsenti, P.L.; Charette, P.G.; Morris, D.; Canva, M. Improved two-temperature modeling of ultrafast thermal and optical phenomena in continuous and nanostructured metal films. *Phys. Rev. B* **2020**, *102*, 155127. [CrossRef]
16. Cesaria, M.; Caricato, A.P.; Beccaria, M.; Perrone, A.; Martino, M.; Taurino, A.; Catalano, M.; Resta, V.; Klini, A.; Gontad, F. Physical insight in the fluence-dependent distributions of Au nanoparticles produced by sub-picosecond UV pulsed laser ablation of a solid target in vacuum environment. *Appl. Surf. Sci.* **2019**, *400*, 330–340. [CrossRef]
17. Gan, R.; Fan, H.; Wei, Z.; Liu, H.; Lan, S.; Dai, Q. Photothermal Response of Hollow Gold Nanorods under Femtosecond Laser Irradiation. *Nanomaterials* **2019**, *9*, 711. [CrossRef]
18. Lombard, J.; Biben, T.; Merabia, S. Nanobubbles around plasmonic nanoparticles: Thermodynamic analysis. *Phys. Rev.* **2015**, *E91*, 043007. [CrossRef]
19. Aibusha, A.V.; Astaf'eva, A.A.; Gosteva, F.E.; Denisovb, N.N.; Titova, A.A.; Shelaeva, I.V.; Shakhova, A.M.; Nadtochenko, V.A. Pulse Heating of Water at the Surface of Gold Nanoparticles: Femtosecond Laser Spectroscopy of Energy Relaxation of Aqueous Colloid of Plasmonic Nanoparticles under Strong Excitation Conditions. *High Energy Chem.* **2015**, *49*, 336–340. [CrossRef]
20. Morris, J.; Dobson, J. *Small Animal Oncology*; Blackwell Science Ltd.: Oxford, UK, 1991.
21. Draine, B.T.; Flatau, P.J. User guide for the discrete dipole approximation code DDSCAT 7.3. *arXiv* **2013**, arXiv:1002.1505.
22. Carpenter, M.; Kennedy, C.A. *Fourth-Order 2N-Storage Runge-Kutta Schemes*; NASA: Washington, DC, USA, 1994; p. 24.
23. Kurisaki, K.; Tanaka, S.; Mori, I.; Umegaki, T.; Mori, Y.; Tanaka, S. Thermal conductivity and conductance of protein in aqueous solution: Effects of geometrical shape. *J. Comput. Chem.* **2023**, *44*, 857–868. [CrossRef]
24. DeLunaa, F.; Cadenaa, M.; Wang, B.; Sun, L.S.; Yea, J.Y. Cellular Refractive Index Comparison of Various Prostate Cancer and Noncancerous Cell Lines via Photonic-Crystal Biosensor. *Proc. SPIE Int. Soc. Opt. Eng.* **2019**, *10881*, 2507505.
25. Elblbesy, M.M. The refractive index of human blood measured at the visible spectral region by single-fiber reflectance spectroscopy. *AIMS Biophys.* **2020**, *8*, 57–65. [CrossRef]
26. Bacallao, R.; Sohrab, S.; Phillips, C. Guiding Principles of Specimen Preservation for Confocal Fluorescence Microscopy. In *Handbook of Biological Confocal Microscopy*, 3rd ed.; Pawley, J.B., Ed.; Springer: Boston, MA, USA, 2006; pp. 368–380.
27. Ding, H.; Lu, J.Q.; Wooden, W.A.; Kragel, P.J.; Hu, X.-H. Refractive indices of human skin tissues at eight wavelengths and estimated dispersion relations between 300 and 1600 nm. *Phys. Med. Biol.* **2006**, *51*, 1479–1489. [CrossRef] [PubMed]
28. Gutiérrez-Varela, O.; Merabia, S.; Santamaria, R. Size-dependent effects of the thermal transport at gold nanoparticle-water interfaces. *J. Chem. Phys.* **2022**, *157*, 0096033. [CrossRef] [PubMed]
29. Chen, X.; Munjiza, A.; Wen, K.Z.D. Molecular Dynamics Simulation of Heat Transfer from a Gold Nanoparticle to a Water Pool. *J. Phys. Chem. C* **2014**, *118*, 1285–1293. [CrossRef]
30. Anderson, A.M.; Anderson, B.E.; Baker, B.A.; Blotter, J.D.; Bramfitt, B.L.; Brown, R.E.; Bruno, B.A.; Collins, P.; Collins, J.A.; Daniewicz, S.R.; et al. *Mechanical Engineers' Handbook*, 4th ed.; Kurz, M., Ed.; John Wiley & Sons, Inc.: Hoboken, NJ, USA, 2015; Volume 1.